JOURNAL OF SCIENCE
SAKARYA UNIVERSITY

Sakarya University Journal of Science

ISSN 1301-4048 | e-ISSN 2147-835X | Period Bimonthly | Founded: 1997 | Publisher Sakarya University | http://www.saujs.sakarya.edu.tr/

Title: Full Order Symbolic Small Signal Analysis of Peak-Current-Controlled SEPIC by PWM-Switch Model

Authors: Ekrem Çengelci
Recieved: 2019-07-02 14:26:36

Accepted: 2019-10-21 22:32:51

Article Type: Research Article
Volume: 24
Issue: 1
Month: February
Year: 2020
Pages: 121-133

How to cite
Ekrem Çengelci; (2020), Full Order Symbolic Small Signal Analysis of Peak-Current-Controlled SEPIC by PWM-Switch Model. Sakarya University Journal of Science, 24(1), 121-133, DOI: 10.16984/saufenbilder.585574
Access link
http://www.saujs.sakarya.edu.tr/tr/issue/49430//585574

Sakarya University Journal of Science 24(1), 121-133, 2020

Full Order Symbolic Small Signal Analysis of Peak-Current-Controlled SEPIC by PWM-Switch Model

Ekrem Çengelci[1]

Abstract

Full order small signal analysis of peak-current controlled non-isolated Single Ended Primary Inductor Converter (SEPIC) is presented by utilizing pwm-switch model in Continuous Conduction Mode (CCM). The analysis provides control to output voltage transfer function together with its zeros and poles in symbolic form taking into account parasitic resistances of all four reactive components in the SEPIC topology. The resultant transfer function is with 4th order numerator and 5th order denominator, which necessitates approximation in deriving formulas of zeros and poles in symbolic form. Symbolically derived transfer function of the SEPIC is validated on two different numerical examples, one with operating in step down mode and another operating in step up mode, by frequency domain PSpice simulations on average circuit models and by time domain LTspice simulations on switching models. The mathematical analysis, PSpice and LTspice simulations, and measurement results of control to output voltage transfer function of SEPIC agree very well proving that the symbolic control to output voltage transfer function of SEPIC together with its zeros and poles are successfully derived.

Keywords: SEPIC, peak current-mode control, pwm-switch, small signal analysis, continuous conduction mode.

1. INTRODUCTION

The SEPIC topology first introduced in [1] as shown in Fig. 1 is used in wide range of applications, such as wind, solar, and fuel cell power conversions, lighting, aerospace and battery. It is one of the dual inductor dc-dc converter topologies that can step up and step down the input voltage. Major advantages of SEPIC are the output voltage polarity being same as that of the input, non-pulsating input current thanks to presence of inductor $L1$ at its input, driving the switch $S1$ being easier since it is a low-side switch.

Current-mode control [2] is a control method of switching dc/dc converters with several advantages [3] such as eliminating phase-lag from control voltage to the switch/inductor current, inherent pulse-by-pulse current limiting protecting the converter against overloads, ease of paralleling converter outputs, ease of applying output current feed-forward minimizing output voltage deviations under load transients, inherent sensitivity to static and dynamic variations of input voltage.

A major disadvantage of dc/dc converters with dual inductors, like SEPIC, is the complexity of their small signal transfer functions due to presence of four reactive components in the topology (inductors $L1$, $L2$ and capacitors $C1$, $Cout$ in Fig. 1). The pwm-switch model presented in [4] is convenient in analyzing small signal behavior of switching dc/dc converters in voltage mode control in CCM while [5,6] present pwm-switch model with peak current-

[1] Türkiye Bilimsel ve Teknolojik Araştırma Kurumu, MAM, Türkiye, ORCID: 0000-0002-4938-8961. ekrem.cengelci@tubitak.gov.tr

mode control in CCM, both of which facilitate fully circuit oriented small signal analysis of switching dc/dc converters as opposed the state space averaging technique involving matrix operations [7]. The model in [5,6] is capable of predicting the subharmonic instability of the current loop causing 180˚ phase reversal at half the switching frequency.[8] performs small signal analysis of SEPIC with peak current-mode control in CCM using the pwm-switch model only on a numerical example without providing equations of the control to output voltage transfer function and its zeros and poles in symbolic form.

[9] provides small signal control to output voltage transfer function of SEPIC in symbolic form by state space averaging technique including the para-

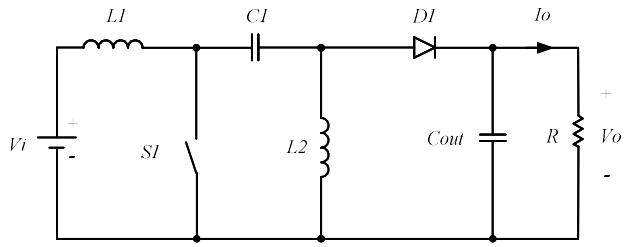

Figure 1. Circuit diagram of non-isolated SEPIC.

sitic resistances of the reactive elements in the topology. However, it neither provides fully expanded control to output voltage transfer function, nor symbolic equations of zeros and poles of the transfer function.

Control to output voltage transfer function of SEPIC in symbolic form is not reported in the literature with constant switching frequency peak current-mode control based on the pwm-switch model including the parasitic resistances of all four reactive elements in the topology and will be presented in this paper. Equations for zeros and poles of the transfer function will be derived in symbolic form with full complexity including the parasitic resistances of the reactive components in SEPIC topology. Symbolic equations provided in the paper enable researchers and engineers to understand effect of each parasitic resistance on the transfer function of the converter. The resultant transfer function and the equations of zeros and poles are too complex for hand manipulations. However, present mathematics software packages, such as Mathcad, Mathematica, Maple, have symbolic arithmetic capabilities that facilitate manipulation of symbolic equations with thousands of parameters with no difficulty. Therefore, once the symbolic transfer function provided in the paper is transferred into a mathematics software, it can be manipulated in its symbolic form by either using it with full complexity or reducing it to a simpler form setting desired parameters to zero by the choice of designer.

Since the derived transfer function is with 4th order numerator and 5th order denominator, equations of the zeros and poles in symbolic form are be derived with approximation assuming locations of zeros and poles are well separated.

2. PWM SWITCH MODEL WITH PEAK CURRENT-MODE CONTROL IN CCM

Pwm-switch models presented in [4], [11]-[14] enable circuit-oriented small signal analysis of switching dc/dc converters. It represents the switch pair in a dc/dc converter with three terminals, which are active terminal “a”, passive terminal “p” and common terminal “c”. The pwm-switch model has dc, large signal and small signal models. Fig. 2 shows significant control signal waveforms, the dc and small signal ac circuit diagrams of the pwm-switch model with peak current-mode control in CCM. In Fig. 2b, upper case voltages and currents represent dc operating point quantities of the converter while lower case ones with tilde accent marks represent small signal ac quantities of the converter. The dc model is utilized to solve for dc operating point quantities while the ac model facilitates to determine the desired small signal transfer function of the dc/dc converter to be analyzed, such as control to output voltage or input to output voltage transfer functions, input or output impedances.

Equations of the pwm-switch model parameters in Fig. 2 are shown in (1a) to (1f).

$$ko = \frac{1}{Ri} \tag{1a}$$

$$go = \frac{Ts}{L} \cdot \left(D' \frac{Se}{Sn} + 0.5 - D \right) \tag{1b}$$

$$gf = D \cdot go - \frac{D \cdot D' \cdot Ts}{2 \cdot L} \tag{1c}$$

$$gi = -\frac{Ia}{Vap} \tag{1d}$$

$$gr = \frac{Ic}{Vap} \tag{1e}$$

$$Cs = \frac{4}{L \cdot \left(\frac{2\pi}{Ts}\right)^2} \tag{1f}$$

where,

Ri is a scaling constant that transforms the "c" terminal current to voltage signal (Ω)

D is the duty cycle in steady state and $D' = 1 - D$,

Ts is the switching period (s),

$$L = \frac{L1 \cdot L2}{L1+L2} \text{ (H)} \quad (2a)$$

$$Sn = \frac{Vac}{L} \cdot Ri \text{ (V/s)} \quad (2b)$$

$$Sf = \frac{Vcp}{L} \cdot Ri \text{ (V/s)} \quad (2c)$$

Se is slope of the external compensation signal (V/s).

Note that Sn is slope of the current coming out of terminal "c" as reflected to the control voltage by the scaling constant Ri. The capacitor Cs in Fig. 2c is to model the subharmonic instability of the current loop [5,6].

The steady state value of control voltage Vc (Fig. 2a) can be solved from (3) given below (see [5,6] for details).

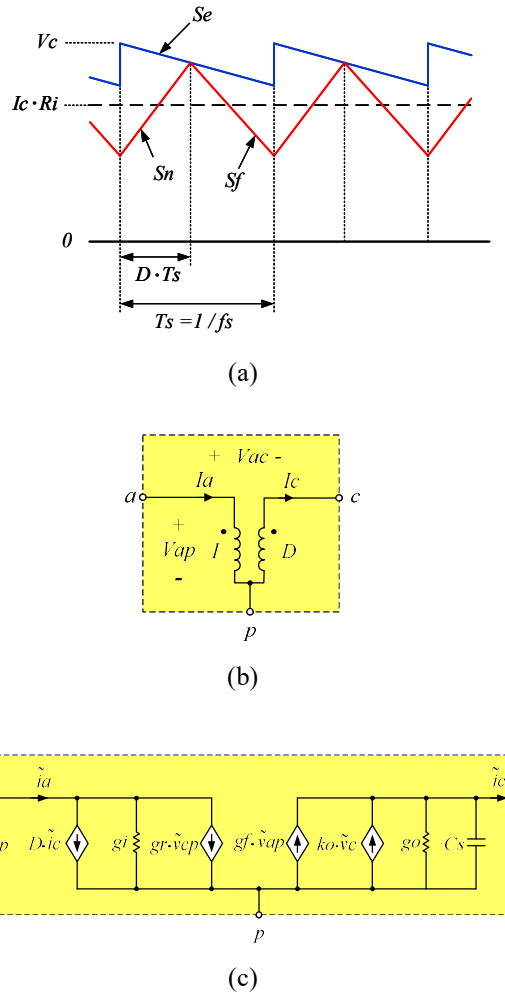

Figure 2. Pwm-switch model with peak current-mode control in CCM (a) Significant control signal waveforms (b) dc equivalent circuit (c) ac equivalent circuit.

$$I_c = \frac{V_c}{R_i} - \frac{V_{cp}}{V_{ap}} \cdot \frac{T_s \cdot S_e}{R_i} - V_{cp} \cdot \left(1 - \frac{V_{cp}}{V_{ap}}\right) \cdot \frac{T_s}{2 \cdot L} \quad (3)$$

3. CONTROL TO OUTPUT VOLTAGE TRANSFER FUNCTION OF SEPIC WITH PEAK CURRENT-MODE CONTROL IN CCM

Switches $S1$ and $D1$ in Fig. 1 are not connected at a common terminal. To carry out the small signal analysis of SEPIC by the pwm-switch model, we need to represent the switch pair $S1$ and $D1$ with three terminals by connecting one of their terminals together. This can be achieved by either moving $D1$ from top to bottom (Fig. 3a) or $C1$ from top to bottom (Fig. 3b). Both works and for the purpose of the analysis of SEPIC in this paper Fig. 3a is chosen for no specific reason.

To solve for the pwm-switch model parameters in (1a) to (1f), we need to obtain dc equivalent circuit of SEPIC by substituting the dc pwm-switch model in Fig. 2b into the switch pair shown within dotted box in Fig. 3a. After shorting capacitors $C1$ and $Cout$ and opening inductors $L1$ and $L2$, the circuit parameters D, Ia, Ic, Vap and Vac in (1b-1e) and (2b, 2c) are solved using the resultant dc equivalent circuit, which is shown in Fig. 4.

If D, Ia, Ic, Vap and Vac are solved from Fig. 4 and substituted into (1b-1e) and (2b, 2c), equations in (4a-4k) can be obtained.

$$\frac{Vo}{Vi} = \frac{D}{1-D} \quad (4a)$$

$$D = \frac{Vo}{Vi + o} \quad (4b)$$

$$Vap = \frac{Vo}{D} \quad (4c)$$

$$Ic = \frac{Vo}{R \cdot (1-D)} \quad (4d)$$

$$Vac = Vi \quad (4e)$$

$$Ia = \frac{Vo}{R} \cdot \frac{D}{(1-D)} \quad (4f)$$

$$Vcp = Vo \quad (4g)$$

$$gi = -\frac{D^2}{R \cdot (1-D)} \quad (4h)$$

$$gr = \frac{D}{R \cdot (1-D)} \quad (4i)$$

$$Sn = Vi \cdot \frac{Ri}{\frac{L1 \cdot L2}{L1+L2}} \quad (4j)$$

$$Sf = Vo \cdot \frac{Ri}{\frac{L1 \cdot L2}{L1+L2}} \quad (4k)$$

Using (3) and (4a-4k) the control voltage Vc can be solved for SEPIC as given in (5).

$$Vc = \frac{Ri \cdot Vo \cdot (1-D)}{2 \cdot L \cdot fs} + \frac{Ri \cdot Io}{(1-D)} + \frac{D \cdot Se}{fs} \quad (5)$$

Now that we have solved for the pwm-switch model parameters for SEPIC as shown in (4a-4k) and (5), next step is to obtain its ac pwm-switch model to derive the transfer function of $\tilde{v}_o/\tilde{v}_c$ by substituting the ac pwm-switch model in Fig. 2c into the switch pair shown within dotted box in Fig. 3a and shorting the dc input voltage source, which results in an equivalent circuit shown in Fig. 5.

Equations in (6a-6g) can be written by applying Kirchhoff's current and voltage laws to the ac equivalent circuit in Fig. 5.

$$\tilde{\imath}a = D \cdot \tilde{\imath}c + \tilde{v}ap \cdot gi + gr \cdot \tilde{v}cp \quad (6a)$$

$$\tilde{\imath}c = \tilde{v}ap \cdot gf + ko \cdot \tilde{v}c - \tilde{v}cp \cdot (go + s \cdot Cs) \quad (6b)$$

$$\tilde{v}cp = \begin{bmatrix} (\tilde{\imath}L1 + \tilde{\imath}c) \cdot (s \cdot L2 + rL2) + \\ (\tilde{\imath}L1 + \tilde{\imath}c + \tilde{\imath}c1) \cdot \frac{R \cdot \left(rC \quad \frac{1}{s \cdot Cout}\right)}{R + \left(rCo \quad \frac{1}{s \cdot Cout}\right)} \end{bmatrix} \quad (6c)$$

$$\tilde{\imath}C1 = \frac{(\tilde{v}ap - \tilde{}o)}{\left(rC1 + \frac{1}{s \cdot C_1}\right)} \quad (6d)$$

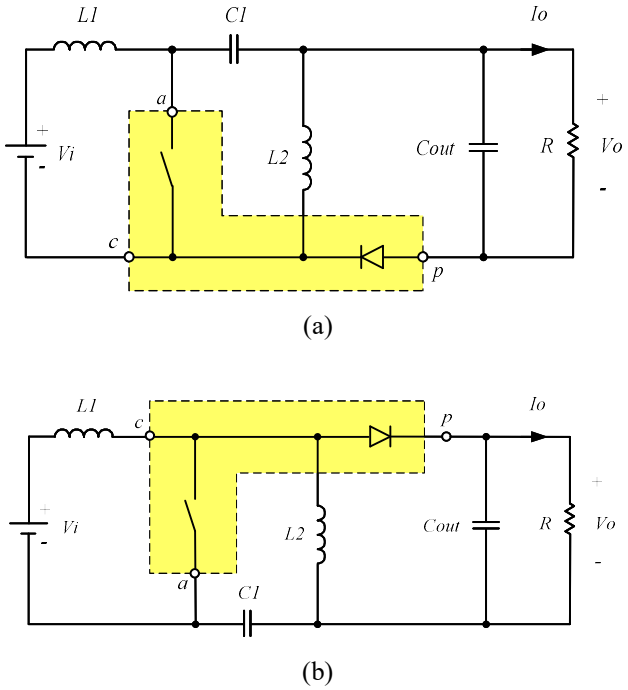

Figure 3. Possible representations of the SEPIC in Fig. 1 by pwm-switch model.

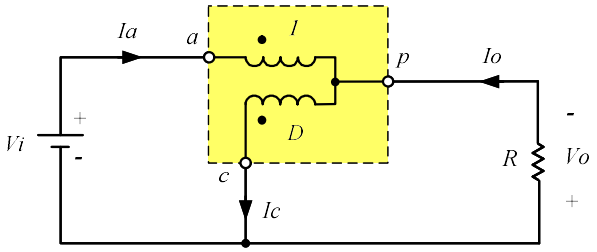

Figure 4. Dc pwm-switch equivalent circuit of the SEPIC in Fig. 3a.

$$\tilde{v}ap = \tilde{v}cp + \tilde{\imath}L1 \cdot (s \cdot L1 + rL1) \quad (6e)$$

$$\tilde{\imath}L1 = -\left(\tilde{\imath}a + \frac{\tilde{v}ap - \tilde{}o}{rC1 + \frac{1}{s \cdot C1}}\right) \quad (6f)$$

$$\tilde{v}o = \left(\tilde{\imath}L1 + \tilde{\imath}c + \frac{\tilde{v}ap - \tilde{v}o}{rC1 \quad \frac{1}{s \cdot C1}}\right) \cdot \frac{R \cdot \left(rCout \quad \frac{1}{s \cdot Cout}\right)}{R + \left(rCout + \frac{1}{s \cdot Cout}\right)} \quad (6g)$$

If the equations in (6a-6g) are simultaneously solved, $\tilde{v}_o/\tilde{v}_c$ can be derived and organized as shown in (7).

$$\frac{\tilde{v}o}{\tilde{v}c} = -R \cdot ko \cdot \frac{N0 + N1 \cdot s + N2 \cdot s^2 + N3 \cdot s^3 + N4 \cdot s^4}{D0 + D1 \cdot s + D2 \cdot s^2 + D3 \cdot s^3 + D4 \cdot s^4 + D5 \cdot s^5} \quad (7)$$

The numerator coefficients $N0$ to $N4$ and denominator coefficients $D0$ to $D5$ in (7) are given in Table 4 in Appendix. The pwm-switch model parameters ko, go, gf, gi, gr, Cs in Table 4 are given in (1) and (4). The denominator of (7) is 5th order because there are five reactive components of $C1$, $Cout$, $L1$, $L2$, and Cs in the ac equivalent circuit of SEPIC in Fig. 5.

Reorganizing the numerator of (7) yields (8) as follows:

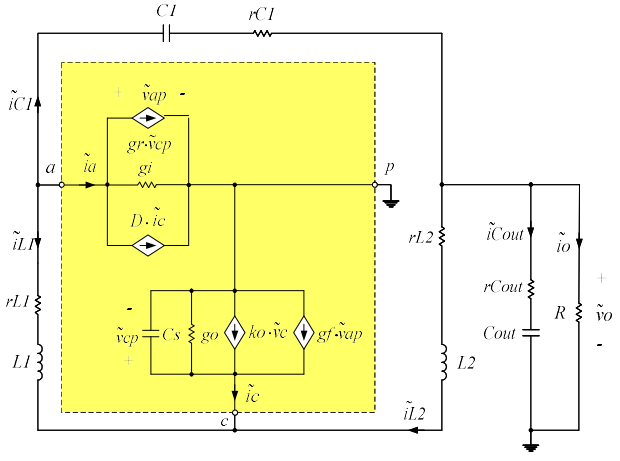

Figure 5. Ac small signal pwm-switch model of the SEPIC.

$$\frac{\tilde{v}o}{\tilde{v}c} = -R \cdot ko \cdot \frac{\left(1 + \frac{s}{\omega z1}\right) \cdot (M0 + M1 \cdot s + M2 \cdot s^2 + M3 \cdot s^3)}{D0 + D1 \cdot s + D2 \cdot s^2 + D3 \cdot s^3 + D4 \cdot s^4 + D5 \cdot s^5} \quad (8)$$

where,

$$\omega z1 = \frac{1}{Cout \cdot rCout} \quad (9a)$$

$$M0 = 1 - D + gi \cdot rL1 \quad (9b)$$

$$M1 = gi \cdot (L1 + C1 \cdot rC1 \cdot rL1) + C1 \cdot \begin{bmatrix} (rC1 + rL2) \cdot (1 - D) + \\ rL1 \cdot (1 - D - gr \cdot rL2) \end{bmatrix} \quad (9c)$$

$$M2 = C1 \cdot \begin{bmatrix} L2 \cdot (1 - D - gr \cdot rL1) + \\ L1 \cdot (1 - D + gi \cdot rC1 - gr \cdot rL2) \end{bmatrix} \quad (9d)$$

$$M3 = -C1 \cdot gr \cdot L1 \cdot L2 \quad (9e)$$

The 3rd order polynomial in the numerator of (8) can be assumed to have a real and a complex pole pair as shown in (10).

$$\begin{pmatrix} M0 + \\ M1 \cdot s + \\ M2 \cdot s^2 + \\ M3 \cdot s^3 \end{pmatrix} = \left(1 + \frac{s}{\omega z2}\right) \cdot \begin{pmatrix} 1 + \\ \frac{s}{\omega o,z \cdot Qz} + \\ \frac{s^2}{(\omega o,z)^2} \end{pmatrix} \quad (10)$$

Exact numeric solutions exist for $\omega z2$, $\omega o,z$, and Qz in (10) but exact symbolic solutions don't. However, approximate symbolic solutions for $\omega z2$, $\omega o,z$, and Qz can only be found by assuming that $\omega z2$ and $\omega o,z$ are well-separated [10].

If $\omega z2 \gg \omega o,z$, then approximate solution of $\omega z2$, $\omega o,z$ and Qz are,

$$\omega z2 \cong \frac{M2}{M3} = -\frac{\begin{matrix} L2 \cdot (1 - D - gr \cdot rL1) + \\ L1 \cdot (1 - D + g \cdot rC1 - gr \cdot rL2) \end{matrix}}{gr \cdot L1 \cdot L2} \quad (11a)$$

$$\omega o,z \cong \sqrt{\frac{M0}{M2}} = \sqrt{\frac{1 - D + gi \cdot rL}{C1 \cdot \begin{bmatrix} L2 \cdot (1 - D - gr \cdot rL1) + \\ L1 \cdot (1 - D + gi \cdot rC1 - gr \cdot rL2) \end{bmatrix}}} \quad (11b)$$

$$Qz \cong \frac{\sqrt{M0 \cdot M2}}{M1} = \frac{\sqrt{\begin{pmatrix} 1 - D + \\ gi \cdot rL1 \end{pmatrix} \cdot C1 \cdot \begin{bmatrix} L2 \cdot (1 - D - gr \cdot rL1) + \\ L1 \cdot (1 - D + \\ gi \cdot rC1 - gr \cdot rL2) \end{bmatrix}}}{\begin{matrix} gi \cdot (L1 + C1 \cdot rC1 \cdot rL1) + \\ C1 \cdot \begin{bmatrix} (rC1 + rL2) \cdot (1 - D) + \\ rL1 \cdot (1 - D - gr \cdot rL2) \end{bmatrix} \end{matrix}} \quad (11c)$$

If $\omega z2 \ll \omega o,z$, then approximate solution of $\omega z2$, $\omega o,z$ and Qz are,

$$\omega z2 \cong \frac{M0}{M1} = \frac{\begin{matrix} 1 - D + gi \cdot rL \\ gi \cdot (L1 + C1 \cdot rC1 \cdot rL1) + \\ C1 \cdot \begin{bmatrix} (rC1 + rL2) \cdot (1 - D) + \\ rL1 \cdot (1 - D - gr \cdot rL2) \end{bmatrix} \end{matrix}} \quad (12a)$$

$$\omega o,z \cong \sqrt{\frac{M1}{M3}} = \sqrt{\frac{\begin{matrix} gi \cdot (L1 + C1 \cdot rC1 \cdot rL1) + \\ C1 \cdot \begin{bmatrix} (rC1 + rL2) \cdot (1 - D) + \\ rL1 \cdot (1 - D - gr \cdot rL2) \end{bmatrix} \end{matrix}}{-C1 \cdot gr \cdot L1 \cdot L2}} \quad (12b)$$

$$Qz \cong \frac{\sqrt{M1 \cdot M3}}{M2} = \frac{\sqrt{-\left(\begin{matrix} gi \cdot (L1 + C1 \cdot rC1 \cdot rL1) + \\ C1 \cdot \begin{bmatrix} (rC1 + rL2) \cdot (1 - D) + \\ rL1 \cdot (1 - D - gr \cdot rL2) \end{bmatrix} \end{matrix} \right) \cdot (C1 \cdot gr \cdot L1 \cdot L2)}}{C1 \cdot \begin{bmatrix} L2 \cdot (1 - D - gr \cdot rL1) + \\ L1 \cdot (1 - D + g \cdot rC1 - gr \cdot rL2) \end{bmatrix}} \quad (12c)$$

The denominator of (7) is 5th order yielding five poles. Subharmonic instability of the current loop is included in the pwm-switch model through Cs, whose equation is given in (1f). It can be deducted from (1f) that Cs and the inductors $L1$ and $L2$ place a double-pole at half the switching frequency. The remaining 3 poles of (7) are a low frequency real pole (ωp) and a complex pole pair (with resonant frequency $\omega o,p1$ and quality factor $Qp1$) as shown in (13).

$$\frac{\tilde{v}o}{\tilde{v}c} = K \cdot \frac{\left(1 + \frac{s}{\omega z1}\right) \cdot \left(1 + \frac{s}{\omega z2}\right) \cdot \left(1 + \frac{s}{\omega o,z \cdot Qz} + \frac{s^2}{(\omega o,z)^2}\right)}{\left(1 + \frac{s}{\omega p}\right) \cdot \left(1 + \frac{s}{\omega o,p1 \cdot Qp1} + \frac{s^2}{(\omega o,p1)^2}\right) \cdot \left(1 + \frac{s}{\omega o,p2 \cdot Qp2} + \frac{s^2}{(\omega o,p2)^2}\right)} \quad (13)$$

Exact solutions to poles of the 5th order denominator of (13) can be found numerically but exact symbolic solutions do not exist. Approximate symbolic solutions for ωp, $\omega o,p1$, $Qp1$, $\omega o,p2$, $Qp2$ can only be found by assuming ωp, $\omega o,p1$ and, $\omega o,p2$ are well-separated [10].

If $\omega o,p2 \gg \omega o,p1 \gg \omega p$, then approximate solutions of ωp, $\omega o,p1$ and $Qp1$, $\omega o,p2$ and $Qp2$ are,

$$\omega p \cong \frac{D0}{D1} \quad (14a)$$

$$\omega o,p1 \cong \sqrt{\frac{D1}{D3}} \quad (14b)$$

$$Qp1 = \frac{\sqrt{D1 \cdot D3}}{D2} \quad (14c)$$

$$\omega o,p2 \cong \sqrt{\frac{D3}{D5}} \quad (14d)$$

$$Qp2 = \frac{\sqrt{D3 \cdot D5}}{D4} \quad (14e)$$

If $\omega o,p2 \gg \omega p \gg \omega o,p1$ then approximate solutions of ωp, $\omega o,p1$ and $Qp1$, $\omega o,p2$ and $Qp2$ are,

$$\omega o,p1 \cong \sqrt{\frac{D0}{D2}} \quad (15a)$$

$$Qp1 = \frac{\sqrt{D0 \cdot D2}}{D1} \quad (15b)$$

$$\omega p \cong \frac{D2}{D3} \quad (15c)$$

$$\omega o,p2 \cong \sqrt{\frac{D3}{D5}} \quad (15d)$$

$$Qp2 = \frac{\sqrt{D3 \cdot D5}}{D4} \quad (15e)$$

The terms from $D0$ to $D5$ in (14a-14e) and (15a-15e) are given in Table 4 in Appendix. Although the high frequency resonant pole of $\omega o,p2$ is expressed in terms of $D0$ to $D5$ in (14a-14e) and (15a-15e) yielding lengthy expression, $\omega o,p2$ is set to half the angular switching frequency by

definition of the PWM-switch model. Therefore, it can be simplified with loss of negligible accuracy as,

$$\omega o, p2 \cong \sqrt{\frac{D3}{D5}} \cong \frac{\omega s}{2} = \pi \cdot fs \quad (16)$$

where fs is the switching frequency of the converter.

The dc gain K in (13) can be found by setting $s = 0$ in (7) as follows:

$$K = -ko \cdot R \cdot \frac{N0}{D0} \quad (17)$$

The equations of poles in (14a-14e) and (15a-15e) are too complex to manipulate manually in symbolic form due to lengthy expressions with the denominator coefficients $D0$ to $D5$ in Table 4. However, present mathematics software packages have capabilities of performing symbolic arithmetic operations. Once the coefficients of (7) in Table 4 are entered into a mathematics software with symbolic arithmetic capabilities, equations of poles in (14a-14e) and (15a-15e) can be manipulated easily and effectively keeping them in full complexity or simplifying them to certain degrees by setting some parameters to zero. This facilitates to analyze the effect of converter parameters on the transfer function in symbolic manner at any complexity level desired.

4. SIMULATION RESULTS

In this section, two different SEPIC's are analyzed, one of which operate in step down mode in Example I and the other in step up mode in Example II. In both examples, control to output voltage transfer functions of the converters are numerically computed using (7) and determined by frequency domain PSpice simulations on average circuit models and by time domain LTspice simulations on switching models. Results of the mathematical model by (7), and LTspice and PSpice simulations are plotted on the same graph for comparison. Since PSpice and mathematical models are both based on pwm-switch model with circuit averaging theory, both are supposed to yield the same transfer function at all frequencies even well above the switching frequency. Therefore, the fact that PSpice simulations of the transfer functions produce the same results as of the mathematical model prove that the symbolic mathematical model parameters in (7) in Table 4 are correctly derived. The transfer function obtained through switching LTspice time domain simulations are not based on circuit averaging. Therefore, the fact that LTspice simulations match the circuit-averaging-based symbolic mathematical model and PSpice simulations proves validity of the circuit averaging based mathematical model by a switching simulation model.

4.1. Example I: A SEPIC operating in step down mode

Consider a SEPIC operating in step down mode with the parameters below.

$Vi = 12V$	$Vo = 5V$	$Io = 5A$
$R = 1\Omega$	$fs = 300kHz$	$\omega s = 1885krad/s$
$Ri = 40m\Omega$	$rCout = 3.5m\Omega$	$Cout = 330\mu F$
$C1 = 82\mu F$	$rC1 = 20m\Omega$	$Se = 40kV/s$
$L1 = 18\mu H$	$L2 = 8.2\mu H$	$rL1 = rL2 = 8m\Omega$

The parameters above are chosen such that the ripple voltages across capacitors $Cout$ and $C1$ are low and ratios of peak-to-peak ripple to average currents of inductors $L1$ and $L2$ are about 30%. Some external slope compensation is assumed (Se) although it is not mandatory for stability of the current loop because the duty cycle is lower than 50%.

Fig. 6 shows the LTspice circuit schematic of the SEPIC with the parameters above with peak-current-mode control. The LTspice simulation model is open loop with the dc voltage source Vc controlling the duty cycle hence output voltage of the converter. Control voltage Vc is calculated as 0.364V using (5) and determined by LTspice simulation as 0.368V (dc voltage source "Vc" in Fig. 6 is varied until output voltage is set to 5V).

Fig. 7 shows the time domain LTspice simulation

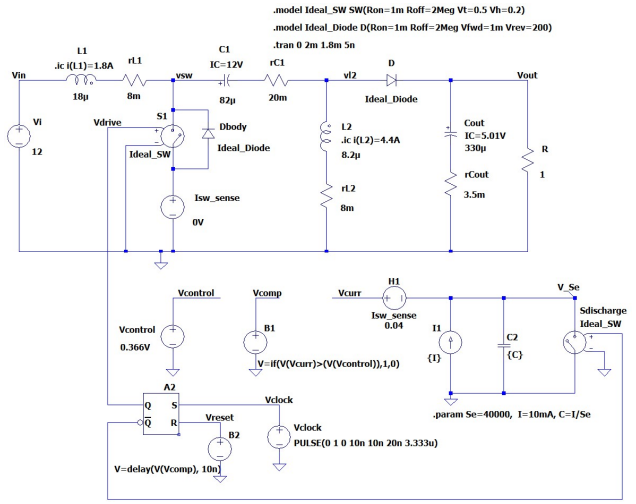

Figure 6. LTspice model of the SEPIC operating in step down mode.

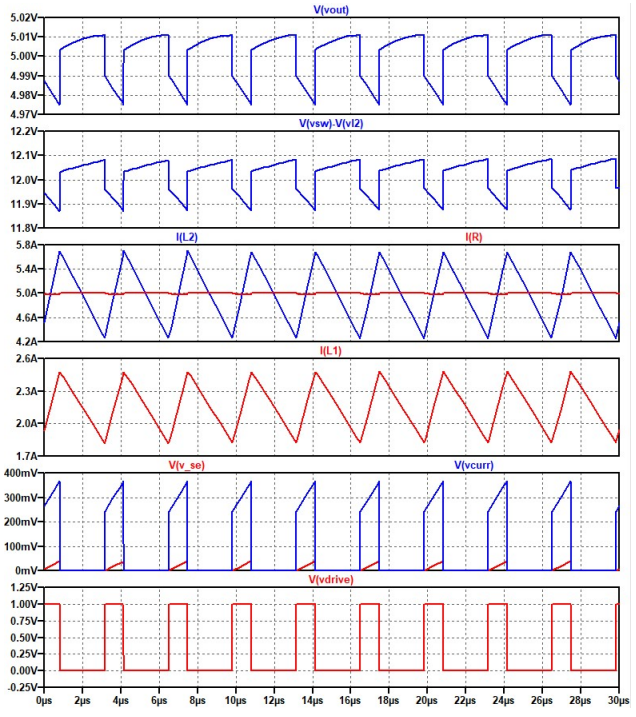

Figure 7. LTspice time domain simulation waveforms of the SEPIC in Fig. 6.

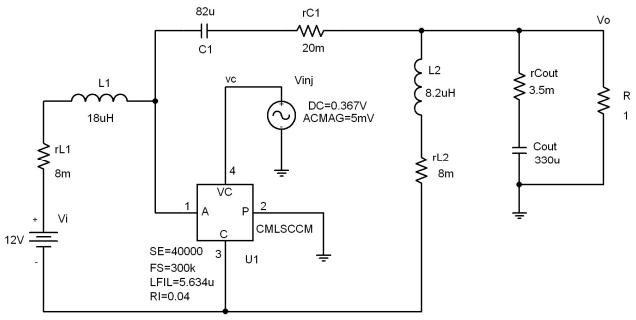

Figure 8. PSpice circuit model of example SEPIC in step-down mode for frequency domain simulation.

waveforms of the SEPIC. From top to bottom, waveforms in Fig. 7 are output voltage, voltage across capacitor C1, current through inductor L2 and load current, current through inductor L1, external slope signal, positive input of the comparator, and logic gate drive signal of the MOSFET.

Table 1. Zeros And Poles of The Transfer Function in (19).

Parameter	Exact Solutions	Approximate Solutions	Unit
$\omega z1$	865.8		$(krad/s)$
$\omega z2$	-300.05	-298.58	
$\omega o,z$	21.583	21.636	
Qz	14.69	258.7	
ωp	4.522	4.422	$(krad/s)$
$\omega o,p1$	21.596	21.716	
$Qp1$	14.55	3.2	
$\omega o,p2$	943.25	948.55	$(krad/s)$
$Qp2$	0.593	0.594	

From (1a-1f), (2a-2c), (4a-4k) and (17), the following parameters can be calculated.

$D = 0.294$ $\quad go = 0.318mho$ $\quad L = 5.634\mu H$

$K = 11.76$ $\quad gi = -0.123mho$ $\quad Sf = 35.5kV/s$

$Cs = 200nF$ $\quad gr = 0.417mho$ $\quad Sn = 85.2kV/s$

$ko = 25mho$ $\quad gf = 0.032mho$

With the parameters of this example SEPIC, the transfer function of $\tilde{v}_o/\tilde{v}_c$ in (7) calculates out as shown in (18).

$$\frac{\tilde{v}o}{\tilde{v}c} = 25 \cdot \frac{\left(\begin{matrix}0.705+6.883\cdot10^{-7}\cdot s+1.506\cdot10^{-9}\cdot s^2\\ -3.304\cdot10^{-1}\ \cdot s^3-5.825\cdot10^{-21}\cdot s^4\end{matrix}\right)}{\left(\begin{matrix}1.499+3.389\cdot10^{-4}\cdot s+4.871\cdot10^{-9}\cdot s^2\\ +7.186\cdot10^{-13}\cdot s^3+1.275\cdot10^{-18}\cdot s^4+\\ 7.986\cdot10^{-2}\ \cdot s^5\end{matrix}\right)} \tag{18}$$

Solving the roots of the numerator and denominator of (18) yields (19) as follows:

$$\frac{\tilde{v}o}{\tilde{v}c} = 11.76 \cdot \frac{\begin{matrix}\left(1+\frac{s}{865.8\cdot10^3}\right)\cdot\left(1+\frac{s}{734.7-21.57\cdot10^3\cdot j}\right)\cdot\\ \left(1+\frac{s}{734.7+21.57\cdot10^3\cdot j}\right)\cdot\left(1+\frac{s}{-30\ \ .05\cdot10^3}\right)\end{matrix}}{\begin{matrix}\left(1+\frac{s}{4.522\cdot10^3}\right)\cdot\left(1+\frac{s}{742.3-21.58\cdot10^3\cdot j}\right)\cdot\\ \left(1+\frac{s}{742.3+21.58\cdot10^3\cdot j}\right)\cdot\\ \left(1+\frac{s}{795.1\cdot10^3-507.48\cdot10^3\cdot j}\right)\cdot\\ \left(1+\frac{s}{795.1\cdot10^3+507.48\cdot10^3\cdot j}\right)\end{matrix}} \tag{19}$$

Angular frequencies of real zeros and poles, resonant angular frequencies and their quality factors of the complex zeros and poles are calculated from (19) and summarized in column "Exact Solutions" in Table 1.

Note that poles and zeros in 'Exact Solutions" column in Table 1 are well separated so that the approximate equations derived in (11a-11c), (12a-12c), (14a-14e) and (15a-15e) are expected to yield values close to those of exact solutions. In

"Approximate Solutions" column of Table 1, (11a-11c) and (14a-14e) are used instead of (12a-12c) and (15a-15e) since $\omega z2 \gg \omega o,z$ and $\omega o,p2 \gg \omega o,p1 \gg \omega p$. It is It is observed in Table 1 that approximate equations in (11a-11c) and (14a-14e) calculate the parameters with negligible errors except Qz and $Qp1$ thanks to zeros and poles of the converter in this example being well-separated.

It is noticed from Table 1 that the zero $\omega z2$ is on the Right Half Plane (RHP).

For the SEPIC example operating in step down mode, frequency domain simulation of the transfer function $\tilde{v}_o/\tilde{v}_c$ can be performed by PSpice using CMLSCCM model in its library, which is a large signal peak current-mode pwm-switch model in

CCM. The PSpice circuit model of the example SEPIC is shown in Fig. 8 for frequency domain analysis.

A flaw has been discovered in the netlist of PSpice model, CMLSCCM. The capacitor Cs has been connected across the nodes "c" and "p" in its netlist resulting in miscalculation of the phase at frequencies nearly half the switching frequency and above. The correct modeling requires connecting the capacitor Cs across the nodes "ca" and "p" instead. In the PSpice simulations presented in this paper, CMLSCCM model has been corrected accordingly. Frequency domain analysis of the example SEPIC is carried out through PSpice using the circuit model in Fig. 8 and through LTspice using the circuit model in Fig. 6. Fig. 9 compares Bode plots obtained through LTspice and PSpice simulations as well as the transfer function in (18). Gain and Phase plots of PSpice simulation and the transfer function in (18), labelled as "Analysis", match perfectly in Fig. 9 even well above the switching frequency expectedly because both CMLSCCM PSpice model and the transfer function in (18) are based on average peak current-mode pwm-switch model in CCM. This proves that the symbolic transfer function in (7) and its coefficients in Table 4 are derived successfully.

The LTspice Bode plots in Fig. 9 are very well in agreement with those of the PSpice simulation and transfer function in (18) but deviate starting at nearly half the switching frequency and above due to the effect of switching with the LTspice circuit model.

As observed in "Exact Solutions" column in Table 1, the angular resonant frequencies of the double zeros and double poles ($\omega o,z$ and $\omega o,p1$) and their quality factors (Qz and $Qp1$) are nearly equal. Therefore, they cancel each other in the Bode plots in Fig. 9 yielding smooth gain and phase plots around the angular frequency of $\omega o,z$. The parameters in the "Approximate Solutions"

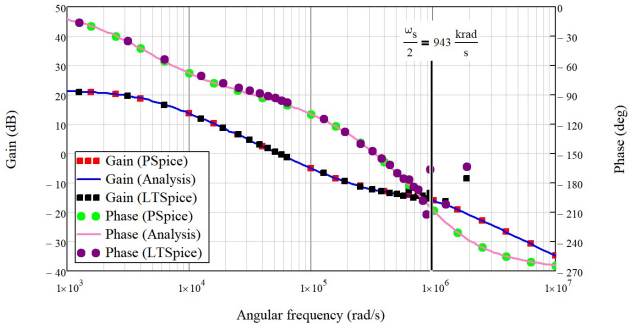

Figure 9. Comparison of Bode plots of $\tilde{v}_o/\tilde{v}_c$ as simulated by LTspice and PSpice and as calculated by the transfer function in (18).

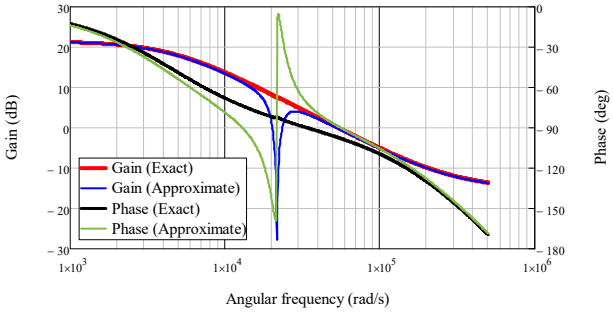

Figure 10. Deviation with gain and phase plots of $\tilde{v}_o/\tilde{v}_c$ around $\omega o,z$ because approximated values of Qz and $Qp1$ differ from their exact values.

column match very well with those in the 'Exact Solutions" column in Table 1 except Qz and $Qp1$, which causes a mismatch with the Bode Plots of exact and approximate solutions around the angular frequency of $\omega o,z$ as shown in Fig. 10.

4.1. Example II: A SEPIC operating in step up mode

Consider a SEPIC operating in step up mode with the following parameters:

$Vi = 12V$	$Vo = 24V$	$Se = 150kV/s$
$R = 8\Omega$	$fs = 400kHz$	$\omega s = 2.512Mrad/s$
$Ri = 50m\Omega$	$Io = 3A$	$Cout = C1 = 100\mu F$
$L1 = 15\mu H$	$rL1 = 12m\Omega$	$rCout = rC1 = 20m\Omega$
$L2 = 10\mu H$	$rL2 = 10m\Omega$	

Parameters of LTspice circuit schematic in Fig. 6 have been updated with the parameters of the SEPIC operating in step up mode. Control voltage Vc is calculated as 0.783V using (5) and determined by LTspice simulation as 0.79V.

Fig. 11 shows the time domain LTspice simulation waveforms of the SEPIC operating in the step up mode. Type and order of waveforms displayed in Fig. 11 are same as those in Fig. 7.

Using (1a-1f), (2a-2c), (4a-4k) and (17), the following parameters can be calculated.

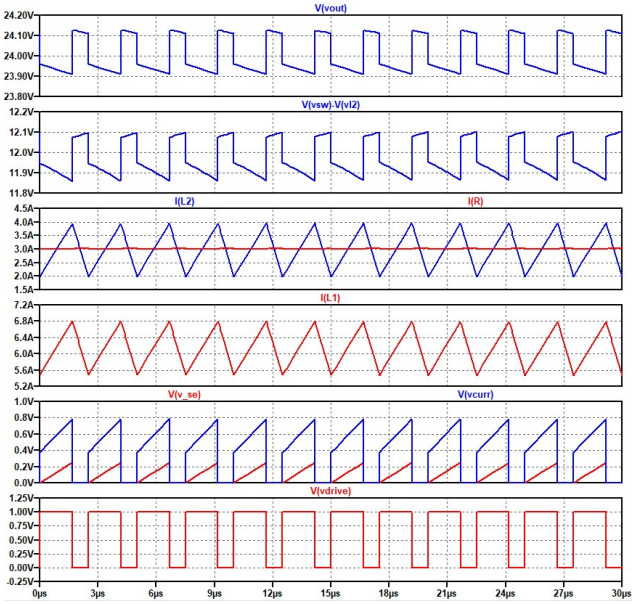

Fig. 11 LTspice time domain simulation waveforms of the SEPIC operating in step up mode.

$D = 0.667$ $go = 0.139mho$ $gr = 0.25mho$

$K = 27.73$ $gi = -0.167mho$ $Sn = 100kV/s$

$L = 6\mu H$ $gf = 0.046mho$ $Cs = 105.5nF$

$ko = 20mho$ $Sf = 200kV/s$

With the parameters of the SEPIC operating in step up mode, the transfer function $\tilde{v}_o/\tilde{v}_c$ in (7) calculates out as shown in (20).

$$\frac{\tilde{v}o}{\tilde{v}c} = 160 \cdot \frac{\left(\begin{matrix}0.331-4.443\cdot10^{-7}\cdot s+8.194\cdot10^{-1}\cdot s^2\\ -2.107\cdot10^{-15}\cdot s^3-7.5\cdot10^{-2}\cdot s^4\end{matrix}\right)}{\left(\begin{matrix}1.912+8.095\cdot10^{-4}\cdot s+7.433\cdot10^{-9}\cdot s^2\\ +2.011\cdot10^{-12}\cdot s^3+1.667\cdot10^{-18}\cdot s^4+\\ 1.261\cdot10^{-24}\cdot s^5\end{matrix}\right)} \tag{20}$$

Solving the roots of the numerator and denominator of (20) yields (21) as follows:

$$\frac{\tilde{v}o}{\tilde{v}c} = 27.73 \cdot \frac{\begin{matrix}\left(1+\frac{s}{500\cdot10^3}\right)\cdot\left(1+\frac{s}{244.1-20.06\cdot10^3\cdot j}\right)\cdot\\ \left(1+\frac{s}{244.1+20.06\cdot10^3\cdot j}\right)\cdot\left(1+\frac{s}{-219.58\cdot10^3}\right)\end{matrix}}{\begin{matrix}\left(1+\frac{s}{2381}\right)\cdot\left(1+\frac{s}{495.6-20.01\cdot10^3\cdot j}\right)\cdot\\ \left(1+\frac{s}{495.6+20.01\cdot10^3\cdot j}\right)\cdot\\ \left(1+\frac{s}{659.12\cdot10^3-1.075\cdot10^6\cdot j}\right)\cdot\\ \left(1+\frac{s}{659.12\cdot10^3+1.075\cdot10^6\cdot j}\right)\end{matrix}} \tag{21}$$

Angular frequencies of real zeros and poles, and resonant angular frequencies and their quality factors of the complex zeros and poles are calculated from (21) and summarized in column "Exact Solutions" in Table 2.

Like in the case of the previous SEPIC example operating in step down mode, poles and zeros in 'Exact Solutions" column in Table 2 are well separated with the SEPIC example operating in step up mode so that the parameter values in the "Approximate Solutions" column calculated using (11a-11c) and (14a-14e) are very close to those of

Table 2. Zeros And Poles of The Transfer Function In (21).

Parameter	Exact Solutions	Approximate Solutions	Unit
$\omega z1$	500		$(krad/s)$
$\omega z2$	-219.58	-219.09	
$\omega o,z$	20.06	20.08	
Qz	41.09	14.9	
ωp	2.381	2.362	$(krad/s)$
$\omega o,p1$	20.012	20.06	
$Qp1$	20.19	5.43	
$\omega o,p2$	1.261	1.263	$(Mrad/s)$
$Qp2$	0.956	0.955	

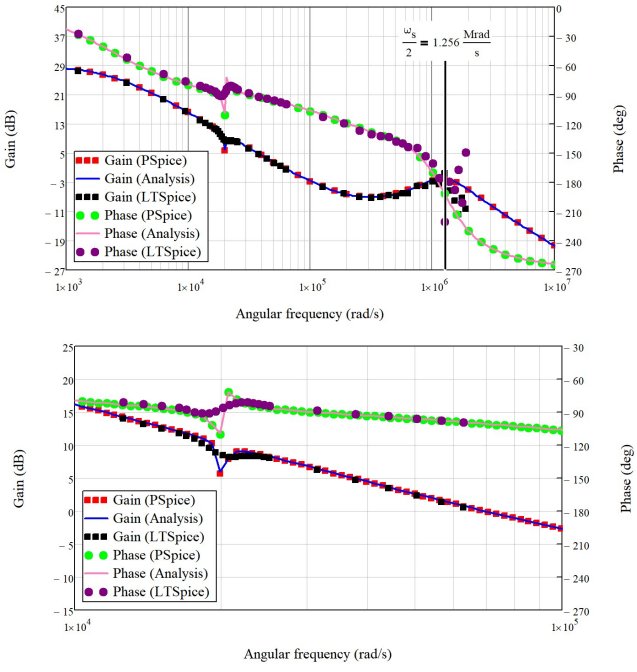

Figure 12. Comparison of Bode plots of $\tilde{v}_o/\tilde{v}_c$ as simulated by LTspice and PSpice and as calculated by the transfer

function in (20). The frequency range on the bottom graph is narrower to show details of the gain and phase plots with sharp changes around $\omega o, z \cong \omega o, p1 \cong 20krad/s$.

the parameters in "Exact Solutions" column except Qz and $Qp1$. (see "Exact Solutions" column in Table 2).

Similar to the SEPIC operating in step down mode, $\omega z2$ in Table 2 is on the RHP, too.

The LTspice simulation model in Fig. 6 and the PSpice simulation model in Fig. 8 are updated with the parameters of the SEPIC example operating in step up mode and frequency domain simulations are carried out with both simulators. Fig. 12 compares the LTspice and PSpice simulation results with the transfer function in (20), labelled as "Analysis". Similar to the plots in Fig. 9, the PSpice simulations and the transfer function in (20) match perfectly at all frequencies even well above switching frequency as expected. LTspice simulation results in Fig. 12 agree very well with the PSpice simulations and the transfer function in (20) up to nearly half the switching frequency and

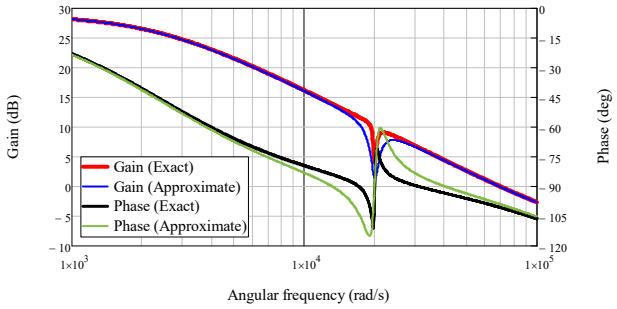

Figure 13. Bode plots of $\tilde{v}_o/\tilde{v}_c$ with exact and approximate solutions in Table 2. The mismatch in Bode plots around $\omega o, z \cong \omega o, p1 \cong 20krad/s$ is due to difference between exact and approximate values of Qz and $Qp1$ in Table 2.

deviate above that due to the switching effect with the LTspice simulation model. There is sudden phase change around the frequency of $\omega o, z \cong \omega o, p1$ this is because Qz and $Qp1$ differ in value (see "Exact Solutions" column in Table 2).

Because of the fact that exact and approximate values do not match in Table 2 for Qz and $Qp1$, the Bode plots generated using the values in exact and approximate values differ in the vicinity of $\omega o, z \cong \omega o, p1$. This mismatch is shown in Fig. 13.

As seen in both examples of SEPIC operating in step up and step down modes, the LTspice and PSpice simulations and the symbolic transfer function in (7) agree very well validating the mathematical analysis of SEPIC with current-mode control in CCM presented in this paper.

5. EXPERIMENTAL RESULTS

LT3759 controller by Analog Devices Inc. has been used for experimental verification. A demo board of LT3759 (part number: DC1787A) has been modified as shown in Table 3. Transfer function $\tilde{v}_o/\tilde{v}_c$ has been measured using frequency response analyzer PSM1735 by Newtons4th Ltd. See Fig. 14 for the picture of the experimental set up.

The output voltage, output current and switching frequency of the converter are set to 12V, 1A and 300kHz, respectively. Experimental tests are carried out with the converter operating in step up mode with $Vi = 9V$ and in step down mode with $Vi = 18V$.

As seen in Fig. 15, the calculated transfer function in (7) and measured transfer function match well.

Table 3 Components Used On the Demo Board Of LT3759

Reference Designator	Component Value	Manufacturer and Part Number
$C1$, $Cout$	$C = 100\mu F$, $esr = 0.25\Omega$	Panasonic Corp., EEU-EB1V221B
$L1$, $L2$	$L = 33\mu H + 47\mu H$ $DCR = 67m\Omega + 68m\Omega$	Viking Tech Corp. PCS127-T330 and PCS127-T470 connected in series
$D1$	3A Schottky Diode	Diodes Inc. PDS360-13
$S1$	60V, 7mΩ, N-Ch. MOSFET	Renesas Elec. Corp., RJK0652DPB-00-J5
Ri	5mΩ, 1/2W, 1%	Vishay Inc., WSL20105L000FEA

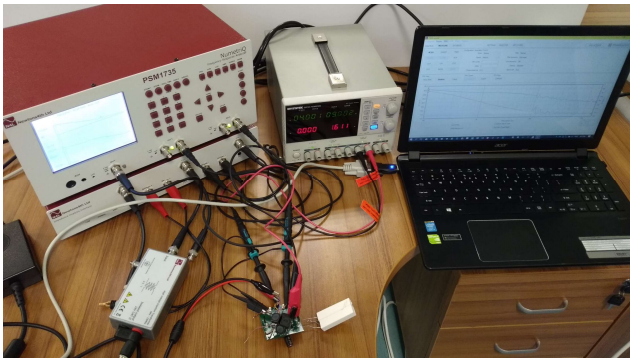

Figure 14. Picture of the experimental set up.

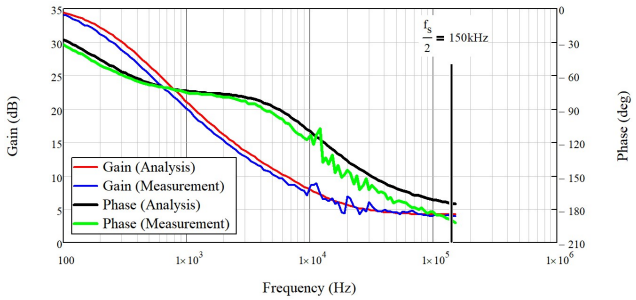

(a) Step down mode, $(Vi = 18V)$.

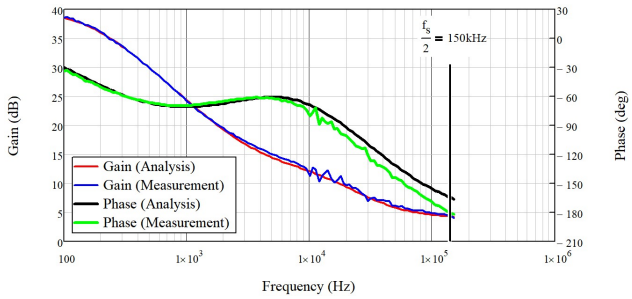

(b) Step up mode, $(Vi = 9V)$

Figure 15. Comparison of calculated and measured Bode Plots of transfer function $\tilde{v}_o/\tilde{v}_c$ in step up and step down modes.

6. CONCLUSIONS

Full order small signal analysis of peak-current controlled non-isolated SEPIC is presented in CCM using the pwm-switch model. Control to output voltage transfer function together with its zeros and poles are provided in symbolic form including parasitic resistances of all four reactive components in the SEPIC. Approximated symbolic transfer functions for zeros and poles of the transfer function are derived with the assumption that zeros and poles are well-separated. Control to output voltage transfer function presented in the paper is validated on two numerical examples operating in step down and step up modes by both frequency domain simulations and switching time domain simulations. It has been shown that the mathematical transfer function derived matches very well with the PSpice frequency domain simulations and LTspice switching time domain simulations, as well as the measurement results. LT3759 controller by Analog Devices Inc. has been used for experimental verification. Measurements have been carried out with the converter operating in both buck and boost modes. Like the simulations results, measurement results also validate the mathematical analysis of the SEPIC transfer function provided in the paper. Since the symbolic equations provided in the paper are derived including the parasitic resistances of all four reactive components in SEPIC, they enable researchers and engineers to understand effect of all these parasitic resistances on the transfer function of the converter. On the other hand, they make the resultant transfer function and the equations of zeros and poles too complex for hand manipulations. Present mathematics software packages have symbolic arithmetic capabilities that facilitate manipulation of symbolic equations with thousands of parameters with no difficulty. Therefore, once the symbolic transfer function provided in the paper is transferred into a mathematics software, it can be manipulated in its symbolic form by either using it with full complexity or reducing it to a simpler form setting desired parameters to zero by the choice of designer.

7. APPENDIX

Table 4 Coefficients of The Transfer Function in (7).

$N0 = 1 - D + gi \cdot rL1$
$N1 = gi \cdot (L1 + C1 \cdot rC1 \cdot rL1 + Cout \cdot rCout \cdot rL1) + (1 - D) \cdot (Cout \cdot rCout + C1 \cdot (rC1 + rL1)) + C1 \cdot (1 - D - gr \cdot rL1) \cdot rL2$
$N2 = Cout \cdot gi \cdot L1 \cdot rCout + C1 \cdot [L2 - gr \cdot L2 \cdot rL1 + L1 \cdot (1 - D + gi \cdot rC1 - gr \cdot rL2) + Cout \cdot rCout \cdot (rC1 + rL1 + gi \cdot rC1 \cdot rL1 + rL2 - gr \cdot rL1 \cdot rL2) - D \cdot (L2 + Cout \cdot rCout \cdot (rC1 + rL1 + rL2))]$
$N3 = C1 \cdot [Cout \cdot rCout \cdot ((1 - D) \cdot (L1 + L2) + gi \cdot L1 \cdot rC1) - gr \cdot (Cout \cdot L2 \cdot rCout \cdot rL1 + L1 \cdot (L2 + Cout \cdot rCout \cdot rL2))]$
$N4 = -C1 \cdot Cout \cdot gr \cdot L1 \cdot L2 \cdot rCout$
$D0 = -1 - [go \cdot (1 - D) + gr] \cdot (R + rL2) - gi \cdot (R + rL1 + go \cdot R \cdot rL1 + rL2 + go \cdot rL1 \cdot rL2) - gf \cdot \begin{bmatrix} D \cdot rL1 - R \cdot ((1 - D) - gr \cdot rL1) - \\ (1 - D - gr \cdot rL1) \cdot rL2 \end{bmatrix}$
$D1 = -(gi \cdot L1) + gf \cdot L2 - gi \cdot L2 - go \cdot L2 - gr \cdot L2 - (Cout + Cs) \cdot R - gi \cdot go \cdot L1 \cdot R - gf \cdot gr \cdot L1 \cdot R - C1 \cdot rC1 + C1 \cdot gf \cdot R \cdot rC1 - C1 \cdot gi \cdot R \cdot rC1 - C1 \cdot go \cdot R \cdot rC1 - C1 \cdot gr \cdot R \cdot rC1 - Cout \cdot rCout + Cout \cdot gf \cdot R \cdot rCout - Cout \cdot gi \cdot R \cdot rCout - Cout \cdot go \cdot R \cdot rCout - Cout \cdot gr \cdot R \cdot rCout - C1 \cdot rL1 - gi \cdot go \cdot L2 \cdot rL1 - gf \cdot gr \cdot L2 \cdot rL1 + C1 \cdot gf \cdot R \cdot rL1 - C1 \cdot gi \cdot R \cdot rL1 - Cout \cdot gi \cdot R \cdot rL1 - Cs \cdot gi \cdot R \cdot rL1 - C1 \cdot go \cdot R \cdot rL1 - C1 \cdot gr \cdot R \cdot rL1 - C1 \cdot gi \cdot rC1 \cdot rL1 - C1 \cdot gi \cdot go \cdot R \cdot rC1 \cdot rL1 - C1 \cdot gf \cdot gr \cdot R \cdot rC1 \cdot rL1 - Cout \cdot gi \cdot rCout \cdot rL1 - Cout \cdot gi \cdot go \cdot R \cdot rCout \cdot rL1 - Cout \cdot gf \cdot gr \cdot R \cdot rCout \cdot rL1 - rL2 \cdot [Cs + gi \cdot go \cdot L1 + gf \cdot gr \cdot L1 + Cs \cdot gi \cdot rL1 + Cout \cdot (R + rCout) \cdot (gi + go + gr + gi \cdot go \cdot rL1 + gf \cdot (-1 + gr \cdot rL1)) + C1 \cdot (1 + (gi + go + gr) \cdot (R + rC1) + go \cdot (1 + gi \cdot (R + rC1)) \cdot rL1 + gf \cdot (R + rC1) \cdot (-1 + gr \cdot rL1))] + D \cdot [Cs \cdot (R + rL2) + go \cdot (L2 + Cout \cdot R \cdot rCout + C1 \cdot R \cdot (rC1 + rL1) + C1 \cdot (R + rC1) \cdot rL2 + Cout \cdot (R + rCout) \cdot rL2) - gf \cdot (L1 + L2 + C1 \cdot (rC1 \cdot (rL1 + rL2) + R \cdot (rC1 + rL1 + rL2)) + Cout \cdot (rCout \cdot (rL1 + rL2) + R \cdot (rCout + rL1 + rL2)))]$
$D2 = -(gi \cdot go \cdot L1 \cdot L2) - gf \cdot gr \cdot L1 \cdot L2 - Cout \cdot D \cdot gf \cdot L1 \cdot R - Cout \cdot gi \cdot L1 \cdot R + Cout \cdot gf \cdot L2 \cdot R - Cout \cdot D \cdot gf \cdot L2 \cdot R - Cout \cdot gi \cdot L2 \cdot R - Cout \cdot go \cdot L2 \cdot R + Cout \cdot D \cdot go \cdot L2 \cdot R - Cout \cdot gr \cdot L2 \cdot R - Cout \cdot D \cdot gf \cdot L1 \cdot rCout - Cout \cdot$

$$gi \cdot L1 \cdot rCout + Cout \cdot gf \cdot L2 \cdot rCout - Cout \cdot D \cdot gf \cdot L2 \cdot rCout - Cout \cdot gi \cdot L2 \cdot rCout - Cout \cdot go \cdot L2 \cdot rCout + Cout \cdot D \cdot go \cdot L2 \cdot rCout - Cout \cdot gr \cdot L2 \cdot rCout - Cout \cdot gi \cdot go \cdot L1 \cdot R \cdot rCout - Cout \cdot gf \cdot gr \cdot L1 \cdot R \cdot rCout - Cout \cdot gi \cdot go \cdot L2 \cdot R \cdot rL1 - Cout \cdot gf \cdot gr \cdot L2 \cdot R \cdot rL1 - Cout \cdot gi \cdot go \cdot L2 \cdot rCout \cdot rL1 - Cout \cdot gf \cdot gr \cdot L2 \cdot rCout \cdot rL1 - Cout \cdot gi \cdot go \cdot L1 \cdot R \cdot rL2 - Cout \cdot gf \cdot gr \cdot L1 \cdot R \cdot rL2 - Cout \cdot gi \cdot go \cdot L1 \cdot rCout \cdot rL2 - Cout \cdot gf \cdot gr \cdot L1 \cdot rCout \cdot rL2 - Cs \cdot [L2 \cdot (1 - D + gi \cdot rL1) + gi \cdot R \cdot (L1 + Cout \cdot rCout \cdot rL1) + gi \cdot (L1 + Cout \cdot (R + rCout) \cdot rL1) \cdot rL2 - Cout \cdot (-1 + D) \cdot (R \cdot rCout + (R + rCout) \cdot rL2)] - C1 \cdot [L2 - gf \cdot L2 \cdot R + D \cdot gf \cdot L2 \cdot R + gi \cdot L2 \cdot R + go \cdot L2 \cdot R - D \cdot go \cdot L2 \cdot R + gr \cdot L2 \cdot R - gf \cdot L2 \cdot rC1 + D \cdot gf \cdot L2 \cdot rC1 + gi \cdot L2 \cdot rC1 + go \cdot L2 \cdot rC1 - D \cdot go \cdot L2 \cdot rC1 + gr \cdot L2 \cdot rC1 + Cout \cdot R \cdot rC1 + Cs \cdot R \cdot rC1 - Cs \cdot D \cdot R \cdot rC1 + Cout \cdot rC1 \cdot rCout - Cout \cdot gf \cdot R \cdot rC1 \cdot rCout + Cout \cdot D \cdot gf \cdot R \cdot rC1 \cdot rCout + Cout \cdot gi \cdot R \cdot rC1 \cdot rCout + Cout \cdot go \cdot R \cdot rC1 \cdot rCout - Cout \cdot D \cdot go \cdot R \cdot rC1 \cdot rCout + Cout \cdot gr \cdot R \cdot rC1 \cdot rCout + go \cdot L2 \cdot rL1 + Cout \cdot R \cdot rL1 + Cs \cdot R \cdot rL1 - Cs \cdot D \cdot R \cdot rL1 + gi \cdot go \cdot L2 \cdot R \cdot rL1 + gf \cdot gr \cdot L2 \cdot R \cdot rL1 + gi \cdot go \cdot L2 \cdot rC1 \cdot rL1 + gf \cdot gr \cdot L2 \cdot rC1 \cdot rL1 + Cout \cdot D \cdot gf \cdot R \cdot rC1 \cdot rL1 + Cout \cdot gi \cdot R \cdot rC1 \cdot rL1 + Cs \cdot gi \cdot R \cdot rC1 \cdot rL1 + Cout \cdot rCout \cdot rL1 - Cout \cdot gf \cdot R \cdot rCout \cdot rL1 + Cout \cdot D \cdot gf \cdot R \cdot rCout \cdot rL1 + Cout \cdot gi \cdot R \cdot rCout \cdot rL1 + Cout \cdot go \cdot R \cdot rCout \cdot rL1 - Cout \cdot D \cdot go \cdot R \cdot rCout \cdot rL1 + Cout \cdot gr \cdot R \cdot rCout \cdot rL1 + Cout \cdot D \cdot gf \cdot rC1 \cdot rCout \cdot rL1 + Cout \cdot gi \cdot rC1 \cdot rCout \cdot rL1 + Cout \cdot gi \cdot go \cdot R \cdot rC1 \cdot rCout \cdot rL1 + Cout \cdot gf \cdot gr \cdot R \cdot rC1 \cdot rCout \cdot rL1 + ((Cs \cdot (1 - D) \cdot (R + rC1)) + Cs \cdot (1 + gi \cdot (R + rC1)) \cdot rL1 + Cout \cdot (rCout + ((-1 + D) \cdot gf + gi + go - D \cdot go + gr) \cdot rC1 \cdot rCout + (go + gi \cdot go \cdot rC1 + gf \cdot gr \cdot rC1) \cdot rCout \cdot rL1 + R \cdot (1 + (gi + go - D \cdot go + gr) \cdot (rC1 + rCout) + go \cdot (1 + gi \cdot (rC1 + rCout)) \cdot rL1 + gf \cdot (rC1 + rCout) \cdot (-1 + D + gr \cdot rL1)))) \cdot rL2 + L1 \cdot [1 + go \cdot R - D \cdot go \cdot R + gr \cdot R + go \cdot rL2 + gi \cdot (R + rC1 + go \cdot R \cdot rC1 + go \cdot (R + rC1) \cdot rL2) + gf \cdot (rC1 \cdot (D + gr \cdot rL2) + R \cdot (-1 + D + gr \cdot (rC1 + rL2)))]]$$

$$D3 = -\big(Cout \cdot (gi \cdot go + gf \cdot gr) \cdot L1 \cdot L2 \cdot (R + rCout)\big) - C1 \cdot [gf \cdot gr \cdot L1 \cdot L2 \cdot (R + rC1) + go \cdot (Cout \cdot L2 \cdot (-((-1 + D) \cdot (rC1 \cdot rCout + R \cdot (rC1 + rCout))) + (rCout + gi \cdot rC1 \cdot rCout + R \cdot (1 + gi \cdot (rC1 + rCout))) \cdot rL1) + L1 \cdot (L2 \cdot (1 + gi \cdot (R + rC1)) + Cout \cdot R \cdot (1 - D + gi \cdot rC1) \cdot rCout + Cout \cdot (R + gi \cdot R \cdot rC1 + rCout + gi \cdot R \cdot rCout + gi \cdot rC1 \cdot rCout) \cdot rL2)) + Cout \cdot (L2 \cdot (rCout + rC1 \cdot rCout \cdot (gi + gr + gf \cdot (-1 + D + gr \cdot rL1)) + R \cdot (1 + (rC1 + rCout) \cdot (gi + gr + gf \cdot (-1 + D + gr \cdot rL1)))) + L1 \cdot (rCout + rC1 \cdot rCout \cdot (D \cdot gf + gi + gf \cdot gr \cdot rL2) + R \cdot (1 + (-gf + gr + gf \cdot gr \cdot rC1) \cdot rCout + D \cdot gf \cdot (rC1 + rCout) + gi \cdot (rC1 + rCout) + gf \cdot gr \cdot (rC1 + rCout) \cdot rL2)))] - Cs \cdot [(Cout \cdot (1 - D) \cdot L2 \cdot (R + rCout)) + C1 \cdot ((Cout \cdot (1 - D) \cdot R \cdot rCout \cdot (rC1 + rL1)) + L2 \cdot (((1 - D) \cdot (R + rC1)) + rL1) + Cout \cdot (((1 - D) \cdot (R \cdot rC1 + (R + rC1) \cdot rCout)) + (R + rCout) \cdot rL1) \cdot rL2 + L1 \cdot (R - D \cdot R + rL2)) + gi \cdot [L1 \cdot (L2 + C1 \cdot R \cdot rC1 + Cout \cdot R \cdot rCout + C1 \cdot (R + rC1) \cdot rL2 + Cout \cdot (R + rCout) \cdot rL2) + rL1 \cdot (Cout \cdot L2 \cdot (R + rCout) + C1 \cdot (L2 \cdot (R + rC1) + Cout \cdot (R \cdot rC1 \cdot rCout + rC1 \cdot rCout \cdot rL2 + R \cdot (rC1 + rCout) \cdot rL2)))]]$$

$$D4 = -(Cout \cdot Cs \cdot gi \cdot L1 \cdot L2 \cdot (R + rCout)) - C1 \cdot [Cout \cdot L1 \cdot L2 \cdot (go \cdot (R + gi \cdot R \cdot rC1 + rCout + gi \cdot R \cdot rCout + gi \cdot rC1 \cdot rCout) + gf \cdot gr \cdot (R \cdot rC1 + (R + rC1) \cdot rCout)) + Cs \cdot [Cout \cdot L2 \cdot (-((-1 + D) \cdot (rC1 \cdot rCout + R \cdot (rC1 + rCout))) + (rCout + gi \cdot rC1 \cdot rCout + R \cdot (1 + gi \cdot (rC1 + rCout))) \cdot rL1) + L1 \cdot [L2 \cdot (1 + gi \cdot (R + rC1)) + Cout \cdot R \cdot (1 - D + gi \cdot rC1) \cdot rCout + Cout \cdot (R + gi \cdot R \cdot rC1 + rCout + gi \cdot R \cdot rCout + gi \cdot rC1 \cdot rCout) \cdot rL2]]]$$

$$D5 = -C1 \cdot Cout \cdot Cs \cdot L1 \cdot L2 \cdot \begin{bmatrix} rCout + gi \cdot rC1 \cdot rCout + \\ R \cdot \big(1 + gi \cdot (rC1 + rCout)\big) \end{bmatrix}$$

REFERENCES

[1] R. P. Massey, E.C. Snyder, "High voltage single-ended DC-DC converter," in Proc. *IEEE PESC*, pp. 156-159, June 1977.

[2] R. Ridley, "A New Small Signal Model for Current Mode Control", Ph.D. Dissertation, ECE Dept., Virginia Institute of Tech., Blacksburg, VA, USA, 1990.

[3] R. Redl, N. Sokal, "Current-mode control, five different types, used with the three basic classes of power converters", in Proc. *IEEE PESC*, pp. 771-785, June 1985.

[4] V. Vorperian, "Simplified analysis of PWM converters using model of PWM switch. Part I: Continuous conduction mode," in *IEEE Trans. Aerospace Electron. Syst.*, vol. 26, issue 3, pp. 490-496, May 1990.

[5] V. Vorperian, "Analysis of Current-Controlled PWM Converters Using the Model of the Current-Controlled PWM Switch," in *PCIM Conference*, pp. 183-195, 1990.

[6] V. Vorperian, "Chapters 8.7 to 8.11" in *Fast Analytical Techniques for Electrical and Electronic Circuits*, 1st ed., Cambridge, United Kingdom, Cambridge University Press, 2002.

[7] R. D. Middlebrook and S. Cuk, "A general unified approach to modeling switching-converter power stages," in Proc. *IEEE PESC*, 1976, pp. 521–570.

[8] W. M. Moussa, "Modeling and performance evaluation of a dc/dc SEPIC converter," in Proc. *IEEE APEC*, pp. 702-706, March 1995.

[9] W. Gu, "Small signal modeling for current mode controlled Cuk and SEPIC converters," in Proc. *IEEE APEC*, pp. 906-910, March 2005.

[10] R.W. Erickson, D. Maksimovic, "Chapter 8.1.8," in *Fundamentals of Power Electronics*, 2nd ed. Boulder, CO, Kluwer Academic Publishers, 2004.

[11] K.D.T. Ngo, "Alternate forms of the PWM switch models," in *IEEE Trans. Aerospace Electron. Syst.*, vol. 35, issue 4, pp. 1283-1292, Oct. 1999.

[12] J. Chen, K.D.T. Ngo, "Alternate forms of the PWM switch model in discontinuous conduction mode," in *IEEE Trans. Aerospace Electron. Syst.*, vol. 37, issue 2, pp. 754-758, Apr. 2001.

[13] V. Vorperian, "Simplified analysis of PWM converters using model of PWM switch. II. Discontinuous conduction mode," in *IEEE Trans. Aerospace Electron. Syst.*, vol. 26, issue 3, pp. 497-505, May 1990.

[14] S. Ben-Yaakov, V. Vorperian "Modeling the switch of PWM convertors (comments, with reply, on 'Simplified analysis of PWM converters using models of PWM switch' by V. Vorperian)," in *IEEE Trans. Aerospace Electron. Syst.*, vol. 28, issue 3, pp. 921-925, July 1992..